Numerical Simulation of Optical Breakdown for Cellular Surgery at Nanosecond to Femtosecond Time Scales

Alfred Vogel* and Joachim Noack**

Medical Laser Center Lübeck, Germany

ABSTRACT

We have shown by experimental investigations that cellular surgery (microdissection, optoporation, and optoinjection) with Nd:YAG laser pulses of 1064 nm and 532 nm wavelength relies on nonlinear absorption leading to optical breakdown and plasma formation at the laser focus. The present study explores possibilities of refining the breakdown effects by employing shorter pulse durations and irradiances that generate plasmas below the threshold for shock wave and bubble formation. Optical breakdown in water at NA = 0.9 and NA = 1.3 was simulated numerically for wavelengths of 1064 nm, 532 nm and 355 nm, and pulse durations of 6 ns, 30 ps and 100 fs. We used a rate equation model that allows the calculation of the temporal evolution of the free electron density r during breakdown. r (t) could be followed separately for the free electrons generated by multiphoton ionization and avalanche ionization. We obtained excellent agreement between the calculated and measured threshold values for breakdown with 6-ns pulses. The simulations predict that the energy threshold for cellular surgery can be reduced by a factor of 350-2600 (depending on wavelength) when the pulse duration is reduced from 6 ns to 100 fs. The calculated breakdown energies for 100 fs pulses focused by an objective with NA = 1.3 are 0.6 nJ at 355 nm, 1.6 nJ at 532 nm, and 3.9 nJ at 1064 nm. With ns-pulses at 1064 nm, the breakdown threshold is very sharp, i. e. there is either no effect at all, or a dense plasma is formed causing a micro-explosion. With shorter wavelengths and pulse durations, the threshold is smoother, and electron densities may be produced that stay below the threshold for explosive vaporization and bubble formation. This creates the possibility of achieving highly localized plasma-mediated chemical or thermal changes in the cell. We conclude that both the reduced energy threshold and the smoother breakdown process with fs pulses bear a large potential for the refinement of intracellular surgery.

Key words: Optical breakdown, plasma formation, cell surgery, microbeam, optoporation, optoinjection, laser dissection, breakdown threshold, multiphoton ionization, avalanche ionization, femtosecond pulses

1. INTRODUCTION

Pulsed laser microirradiation[1-8] is used in cell and molecular biology for single cell preparation, microdissection and inactivation of cell organelles or chromosomes, and molecule and gene transfer through the cell membrane by optoporation or optoinjection. Another application is contamination-free catapulting of dissected cells into the container used for further gene and protein analysis.[4, 7] These methods usually employ nanosecond (ns) pulses at infrared, visible and UV wavelength which are focused on the target by microscope objectives of large numerical aperture (NA).[1-4] Even though the techniques are widely used, the underlying mechanisms are still largely a subject of speculations.

Highly localized energy deposition during pulsed laser microirradiation can be achieved even in media which are nominally transparent at low irradiance. This fact suggests that the energy deposition relies on a nonlinear absorption mechanism through which a large absorption coefficient is created exclusively in those regions where the irradiance is very high. We provided experimental evidence that cellular surgery with Nd:YAG laser pulses of 1064 nm and 532 nm wavelength relies on optical breakdown leading to plasma formation at the laser focus.[9]

The experimental results showed that the expansion of the hot plasma causes strong mechanical effects such as the emission of a shock wave and the formation of a cavitation bubble. The shock wave pressure at the plasma boundary was in the order of 2 GPa, and the cavitation bubble reached a maximum radius of 45 μm or larger when the laser pulses were focused into distilled water.[9] This indicates that cells are subject to large mechanical stresses during pulsed microirradiation which are likely to produce adverse side effects.

* vogel@mll.mu-luebeck.de; phone: xx49-451-500-6504, fax: xx49-451-505 486; http://www.mll.mu-luebeck.de; Medizinisches Laserzentrum Lübeck, Peter-Monnik-Weg 4, 23562 Lübeck, Germany. **Joachim_Noack@hotmail.com

In the present study we explore the possibilities of refining the breakdown effects by employing shorter pulse durations and irradiances below the threshold for shock wave and bubble formation. For that purpose we performed numerical simulations of the optical breakdown process using a rate equation model that allows for the calculation of the breakdown thresholds and the temporal evolution of the free electron density $r(t)$ during breakdown.[10] $r(t)$ was followed separately for the free electrons generated by multiphoton ionization (MPI) and cascade ionization (CI) in order to analyze the interplay of both ionization mechanisms during breakdown. We further calculated the maximum electron density reached during the laser pulse as a function of irradiance. These calculations allow one to assess the sharpness of the breakdown threshold and the possibility of the creation of low density plasmas with an energy density below the threshold for shock wave and bubble formation.

The numerical simulations readily provide an overview over a large parameter range which is difficult to obtain experimentally. We simulated the optical breakdown in water at NA = 0.9 and NA = 1.3 for wavelengths of 1064 nm, 532 nm and 355 nm, and pulse durations of 6 ns, 30 ps and 100 fs.

2. NUMERICAL MODEL

2.1 Optical breakdown

It has been shown that optical breakdown in water is very similar to that in ocular and other biological media[11]. For convenience we shall therefore focus attention on optical breakdown in pure water. Whereas optical breakdown in gases leads to the generation of free electrons and ions, it must be noted that in water electrons are either bound to a particular molecule or they are "quasi-free" if they have sufficient kinetic energy to be able to move without being captured by local potential energy barriers. Transitions between bound and quasi-free states are the equivalent of ionization of molecules in gases. To describe the breakdown process, Sacchi[12] has proposed, therefore, that water should be treated as an amorphous semiconductor and the excitation energy regarded as the energy required for a transition from the molecular $1b_1$ orbital into an excitation band (6.5 eV).[13] We follow this approach. For simplicity, we use the terms "free electrons" and "ionization" as abbreviations for "quasi-free electrons" and "excitation into the conduction band".

At the wavelengths of 1064 nm, 532 nm and 355 nm investigated in this study, the energy of six, three, and two photons, respectively, is required to produce an electron-hole pair (the photon energies at the respective wavelengths are 1.17 eV, 2.34 eV, and 3.51 eV). In pure water, this energy can only be provided by a multiphoton process where several photons interact 'simultaneously' (within a time interval $\Delta t = 2p / w_L$) with a bound electron. The multiphoton ionization rate is proportional to I^k, where I is the laser light irradiance and k the number of photons required for ionization.

Once a free electron exists in the medium, it can absorb photons in a non-resonant process called 'inverse Bremsstrahlung' in the course of collisions with heavy charged particles (ions or atomic nuclei).[14] A third particle (ion/atom) is necessary for energy and momentum to be conserved during absorption, as they cannot be conserved if only an electron and a photon interact. The electron gains kinetic energy during the absorption of a photon and, in a sequence of several such events, the energy gain becomes so large that the electron can produce another free electron through impact ionization. Two free electrons with low kinetic energies are now available and they can again gain energy through inverse Bremsstrahlung absorption. This leads to an avalanche growth in the number of free electrons, provided the irradiance is high enough to overcome the loss of free electrons through diffusion out of the focal volume and through recombination. The energy gain through inverse Bremsstrahlung must, moreover, be more rapid than the energy loss through collisions with heavy particles. (Electron-ion collisions are not entirely elastic, but a small fraction of the electron's energy, proportional to the ratio of the electron and ion masses, will be transferred to the ion). The process is called 'avalanche ionization', or 'cascade ionization'. At very high irradiance, such that the losses can be neglected, the cascade ionization rate is proportional to the irradiance.[15]

While multiphoton ionization is "instantaneous," there are time constraints on cascade ionization because several consecutive inverse Bremsstrahlung absorption events are necessary for a free electron to pick up the kinetic energy required for impact ionization. When the ionization energy is 6.5 eV and the photon energy is, for example, 1.2 eV (λ = 1064 nm), an electron must undergo at least 6 inverse Bremsstrahlung events before impact ionization can occur. As mentioned above, these events can only occur during collisions of the electrons with heavy particles. Bloembergen estimates that in condensed matter the time t between collisions is roughly 1 fs.[16] The process thus requires at least 6 fs, even at extremely high irradiance such that almost every collision involves inverse Bremsstrahlung absorption.

For sufficiently high irradiance, the interplay of multiphoton ionization and cascade ionization leads to an "optical breakdown" during which the material at the laser focus becomes partially or fully ionized. The expression is based on an analogy with electrostatic breakdown, which occurs when very high dc fields are applied to electrical insulators.[16] The threshold for optical breakdown is defined by the irradiance (or energy) required to produce a certain critical free electron density ρ_{cr} at the laser focus. When nano- and picosecond pulses are employed, optical breakdown is accompanied by the formation of a luminous plasma.[17] With shorter laser pulses, on the contrary, there is no plasma luminescence in the visible region of the spectrum, and breakdown can only be detected by observing the formation of a cavitation bubble in the liquid.[10,18] It has been found previously that the critical electron density for optical breakdown in water (corresponding to the thresholds for the formation of a luminous plasma or a cavitation bubble, respectively) is $\rho_{cr} = 10^{20}$ cm^{-3} for ns-pulses and 10^{21} cm^{-3} for ps- and fs-pulses.[10] A physical explanation of the pulse duration dependence of ρ_{cr} is given in Ref. [10].

In order for an ionization cascade leading to plasma formation to occur, a few free electrons ("seed electrons") must be available in the focal volume at the beginning of the laser pulse. In pure water, they can be produced only by multiphoton ionization. Since multiphoton ionization is statistical in character, the breakdown threshold is defined as the irradiance at which plasma formation will be observed with a 50% probability.

2.2 Calculations

We calculated the time evolution of the electron density ρ under the influence of the laser light in order to determine the threshold irradiance required to produce breakdown. The time evolution of the electron plasma can, in a simplified way, be described by a rate equation of the form[10]

$$\frac{d\rho}{dt} = \eta_{mp} + \eta_{casc}\,\rho - g\,\rho - \eta_{rec}\,\rho^2 . \qquad (1)$$

The first two terms represent the production of free electrons through multiphoton and cascade ionization, and the last two the losses through diffusion of electrons out of the focal volume and recombination. The cascade ionization rate η_{casc} and the diffusion loss rate g are proportional to the number of already produced free electrons, while the recombination rate η_{rec} is proportional to ρ^2, as it involves an interaction between two charged particles (an electron-hole pair). For a detailed description of the individual terms of Eq. (1) the reader is referred to references [10] and [19].

The time evolution of the electron density, $\rho(t)$, was calculated for laser pulses with a Gaussian time variation.[10] $\rho(t)$ was followed separately for the free electrons generated by multiphoton ionization and avalanche ionization, and the total free electron density was obtained by adding both contributions. Since free electrons must exist in the interaction volume for cascade ionization to occur, the term for cascade ionization was first included when the free electron density owing to multiphoton ionization has increased to the point where a statistical average of 0.5 electrons exist within the focal volume. Optical breakdown should then follow with 50% probability. The focal volume was assumed to be cylindrical with a diameter equal to the focal diameter d of a Gaussian beam and a length $l = \pi d^2 / 2\,l$ (twice the Rayleigh length). In order to account for the time $t_{ion} = t\,k$ required for an electron to acquire the band gap energy ΔE through inverse Bremsstrahlung absorption and produce another free electron, the contribution of cascade ionization was evaluated using the electron density at time t - t_{ion}. For our calculations, we used a value of t = 1 fs for the time between electron - heavy particle collisions.[16] To determine the irradiance threshold I_{rate} required to produce breakdown for a given wavelength and pulse duration, Eq. (1) was iteratively solved for different irradiance values until the maximum electron density during the laser pulse ρ_{max} equaled the critical density ρ_{cr} for optical breakdown. Following Ref. [10] we used $\rho_{cr} = 10^{20}$ cm^{-3} for a pulse duration of 6 ns, and $\rho_{cr} = 10^{21}$ cm^{-3} for pulse durations of 30 ps and 100 fs. The breakdown energy E_{rate} was calculated by multiplying I_{rate} with the diffraction limited area of the focal spot and the laser pulse duration. To assess the dependence of the maximum electron density on irradiance, ρ_{max} was plotted as a function of I/I_{rate}.

3. RESULTS AND DISCUSSION

3.1 Comparison of calculated and measured breakdown thresholds with parameters used for cell surgery

In Table 1, the calculated breakdown thresholds for 6 ns pulses with 1064 nm and 532 nm wavelength are compared to our experimental results for optical breakdown in distilled water[9] obtained at a numerical aperture of NA = 0.9. The agreement of E_{rate} with E_{th} is very good. In previous investigations a similarly good agreement between calculations and experimental results was found for NA = 0.25 at pulse durations of 6 ns, 30 ps, and 100 fs.[10]

λ (nm)	Calculations		Experiments	
	I_{rate} (10^{11} W cm^{-2})	E_{rate} (μJ)	I_{th} (10^{11} W cm^{-2})	E_{th} (μJ)
532	0.44	1.1	0.77	1.9
1064	1.70	16.6	1.87	18.3

Table 1: Calculated and measured breakdown thresholds for distilled water at NA = 0.9 and 6 ns pulse duration. A diffraction limited spot size was assumed for the calculation of E_{rate} from I_{rate} and I_{th} from E_{th}, respectively. $r_{cr} = 10^{20}$ cm^{-3}.

λ (nm)	Calculated breakdown threshold for water (μJ)	Threshold for optoinjection (μJ)
532	0.5	0.5
1064	10.3	12.0

Table 2: Calculated breakdown thresholds E_{rate} for distilled water at NA = 1.3 and 6 ns pulse duration, compared to the energy thresholds for optoinjection at the same parameters.[6]

In table 2 the calculated energy thresholds for optical breakdown in water at NA = 1.3 are compared to the energies employed in optoinjection, a technique where exogenous molecules are delivered into a single cell via the pulsed irradiation of the cell membrane.[6] The excellent agreement of the energy values suggests that optical breakdown is the working mechanism of optoinjection. Since the energies used for optoporation and laser pressure catapulting are higher than those used for optoinjection, we can conclude that these microirradiation techniques rely also on optical breakdown.

3.2 Dependence of breakdown thresholds on pulse duration and wavelength

Table 3 lists the irradiance thresholds for optical breakdown in water at NA = 1.3 for wavelengths of 1064 nm, 532 nm and 355 nm, and pulse durations of 6 ns, 30 ps and 100 fs. Table 4 summarizes the corresponding energy thresholds which were calculated from the irradiance threshold assuming a diffraction limited spot size.

Pulse duration	r_{cr} (cm^{-3})	I_{rate} (10^{11} W cm^{-2})		
		355 nm	532 nm	1064 nm
6 ns	10^{20}	1.14	0.47	2.19
30 ps	10^{21}	7.76	3.63	2.67
100 fs	10^{21}	68.0	80.6	49.3

Table 3: Calculated irradiance thresholds I_{rate} for optical breakdown in distilled water at NA = 1.3. The values chosen for r_{cr} yielded the best agreement between calculated and measured data in a previous study with NA = 0.25.[10]

Pulse duration	ρ_{cr} (cm^{-3})	E_{rate} (nJ)		
		355 nm	532 nm	1064 nm
6 ns	10^{20}	596	553	10290
30 ps	10^{21}	20.3	21.3	62.7
100 fs	10^{21}	0.59	1.56	3.86

Table 4: Calculated energy thresholds E_{rate} for optical breakdown in distilled water at NA = 1.3.

For all wavelengths investigated, the irradiance threshold increases with decreasing pulse duration (Table 3) because the breakdown process has to be completed within an ever shorter period of time. The increase of irradiance is, however, much less pronounced than the decrease of pulse duration, owing to the nonlinear relationship between ionization rate and irradiance. As a consequence, the energy threshold is reduced by a factor of 2600 at 1064 nm, 350 at 532 nm, and a factor of 1000 at 355 nm, respectively, when the pulse duration is diminished from 6 ns to 100 fs, and the breakdown energies at 100 fs pulse duration are only 0.6 nJ to 3.9 nJ (Table 4). This means that much finer laser effects can be produced with femtosecond pulses than with nanosecond pulses.

It is interesting to note that the breakdown energy predicted for ns- and ps-pulses at 355 nm is not or hardly smaller respectively, than at 532 nm even though the spot size is smaller at the shorter wavelength. The reason is that the increase of the multiphoton ionization rate with shorter wavelengths is compensated by a decrease of the cascade ionization rate with decreasing wavelength.[10]

The use of a diffraction limited spot size for the calculation of E_{rate} implies the assumption that the focal spot is not influenced by self-focusing effects. This assumption is justified by the fact that the highest threshold predicted for the laser power required for breakdown (at τ = 100 fs, λ = 1064 nm) is 3.9×10^4 W, about 50 times lower than the critical power for beam collapse through self-focusing which is 2.4×10^6 W.[20] Self-focusing effects play a role, however, for smaller numerical apertures,[17,20] and they may play a role at large numerical aperture for pulse durations considerably shorter than 100 fs.

3.3 Time evolution of the electron density during plasma formation: Interplay of multiphoton and cascade ionization

A deeper insight in the mechanisms underlying the parameter dependence of the breakdown thresholds can be obtained by looking at the temporal evolution of the electron density, $r(t)$, during breakdown. The $r(t)$ curves in figure 1 reveal the relative importance of multiphoton and cascade ionization and their interplay in the course of breakdown. Multiphoton ionization becomes increasingly important for shorter wavelengths and pulse durations. At short wavelengths, a smaller number of photons is required to provide the ionization energy. At shorter pulse durations, a higher irradiance is necessary for optical breakdown to occur. This favors the generation of free electrons through multiphoton ionization because of its stronger irradiance dependence $\propto I^k$ as opposed to $\propto I$ for the cascade ionization rate (see section 2.1 and Ref [10]).

It is interesting to note that the large majority of free electrons is always created by cascade ionization and not by multiphoton ionization - even for 100 fs pulses at UV wavelengths. The reason is that the cascade ionization rate is proportional to the density of free electrons already produced in the course of the laser pulse, whereas the multiphoton ionization rate is independent of r. The initial part of the breakdown process is, therefore, dominated by multiphoton processes, but this phase lasts only until the number of free electrons is so large that cascade ionization starts to govern the breakdown dynamics.

For most parameters investigated, the breakdown threshold is determined by the irradiance required to produce the critical electron density r_{cr} before the end of the laser pulse, and the increase of the free electron density during the laser pulse is fairly smooth. The situation differs, however, for laser pulses with 1064 nm wavelength and pulse durations of 6 ns or 30 ps. In these cases, the breakdown threshold is defined by the irradiance necessary to generate the start electron for cascade ionization by means of multiphoton ionization. This irradiance is very high for 1064 nm, because 6 photons are required for multiphoton ionization. Once a seed electron has been created, the ionization cascade can start and proceeds very rapidly owing to the high irradiance. The electron density shoots up by 9 orders of magnitude within a small fraction of the laser pulse duration and even overshoots the critical electron density of $r_{cr} = 10^{21}$ cm^{-3}. The ionization cascade is then stopped by recombination processes, because the recombination rate is proportional to r^2 (see Eq. (1)).

The fact that multiphoton-generation of seed electrons constitutes an additional hurdle for optical breakdown at 1064 nm with ns and ps pulses explains the particularly high breakdown threshold at these parameters. The rapidity of the cascade ionization taking place when seed electrons are present explains, furthermore, why the plasma size observed with 6 ns pulses at 1064 nm is much larger than at 532 nm.[9] When the plasma begins to form in the focal volume, the electron-hole recombination results in the emission of radiation at UV wavelengths. The photon energy of this radiation is sufficiently high to produce free electrons in the vicinity of the plasma which can then act as seed electrons for an ionization cascade. Optical breakdown will, therefore, occur in the whole region where the irradiance suffices to complete the breakdown cascade up to the critical electron density. This region can be considerably larger than the focal region if the irradiance for completion of the breakdown cascade is less than the $1/e^2$ part of the irradiance required to produce the initial seed electron.

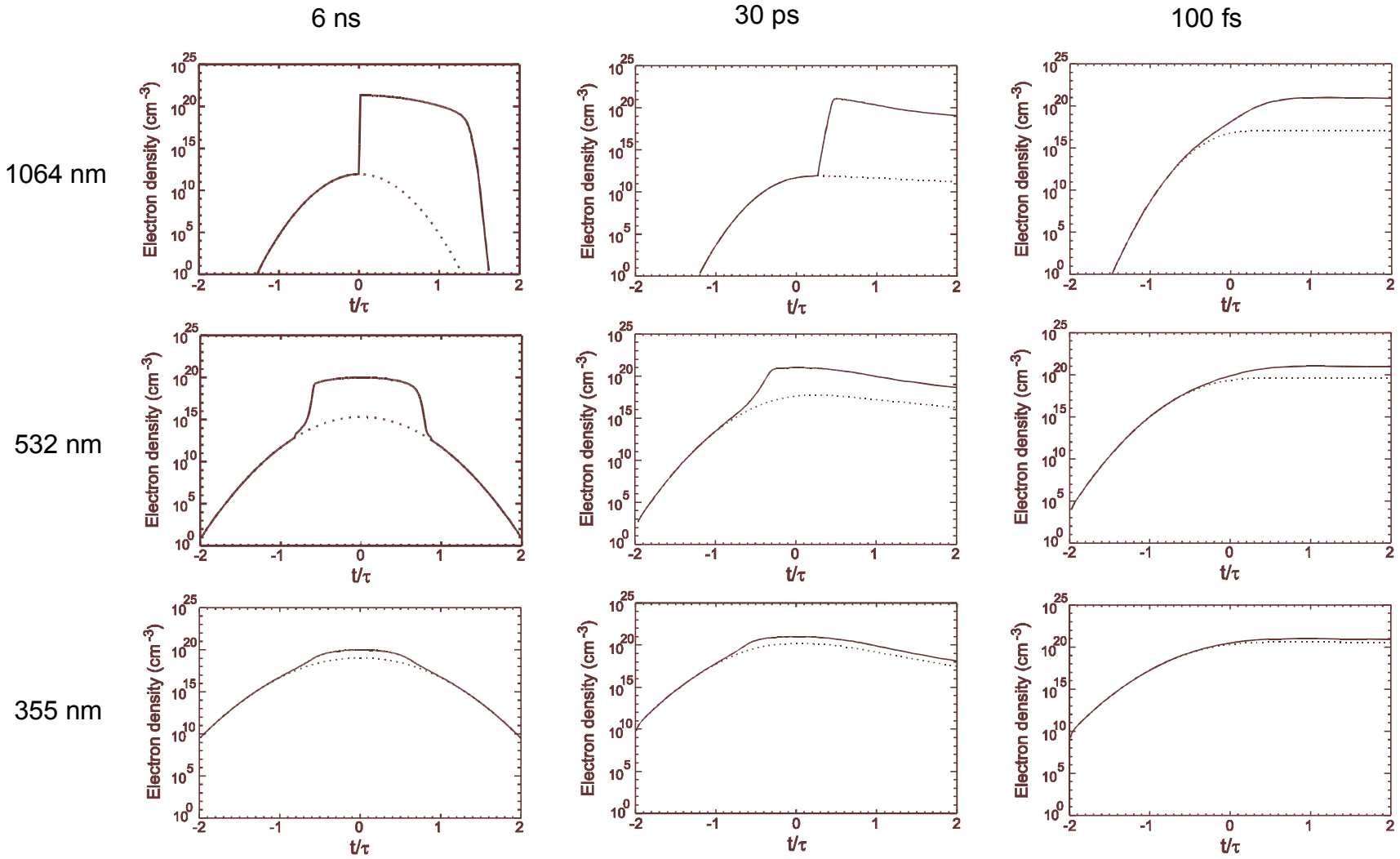

Figure 1: Evolution of the free electron density at breakdown threshold for different pulse durations (left to right) and different wavelengths (top to bottom). The calculations were performed for laser pulses focused into pure water at NA = 1.3. Besides the total free electron density (solid curve), the density due to multiphoton absorption alone (dotted curve) is plotted as a function of time. The time axes have been normalized to the laser pulse duration t_L (FWHM).

Large plasmas at threshold energy have previously also been observed for optical breakdown at l = 1064 nm with numerical apertures NA ≤ 0.25.[17] The growth of the plasma beyond the focal volume is, however, particularly pronounced with large NA where the focal volume is very small (1.15 μm^3 at NA = 1.3, l = 1064 nm). The creation of one seed electron in the focal volume corresponds here to the generation of a free electron density of ≈10^{12} cm^{-3} which requires a particularly high irradiance (I_{rate} is 4.4 times higher at NA = 1.3, l = 1064 nm than at NA = 0.25). The high irradiance causes a stronger enlargement relative to the focal volume than at smaller NA.

3.4 Threshold Sharpness: Dependence of maximum electron density on irradiance

Figure 2 presents plots of r_{max} as a function of I/I_{rate} which allow the assessment of the 'sharpness' of the breakdown threshold. The term 'threshold sharpness' means here the deterministic dependence of maximum electron density on irradiance according to Eq. (1), and should not be confused with the statistic variations owing to the probabilistic nature of breakdown.

The threshold is very sharp in those cases where the breakdown relies on the multiphoton generation of seed electrons for the ionization cascade (6 ns and 30 ps pulses at 1064 nm): if no seed electron is produced, no plasma is created at all, but if only one seed electron is produced, that results already in a very high electron density.

The scenario is very different in cases where multiphoton ionization occurs already at irradiance values considerably below the breakdown threshold (with femtosecond pulses, and longer pulses at UV wavelengths). For a pulse duration of 100 fs and a wavelength of 355 nm, for example, a free electron density of 10^{18} cm^{-3} (i. e. 0.001x r_{cr}) is predicted to be produced at 0.07× I_{rate}. This means that 'low density plasmas' are produced in a fairly large irradiance range below the breakdown threshold. The breakdown threshold is, for femtosecond pulses, defined as lower irradiance limit for the generation of a cavitation bubble at the laser focus. The possibility of producing plasmas with electron densities below r_{cr} implies, therefore, that one can generate laser effects without bubble formation.

To support this interpretation, we shall now estimate the free electron density at which the energy carried by the free electrons is large enough to heat the water to the boiling temperature of 100°C. The total energy carried by a free electron consists of the band gap energy ΔE plus its kinetic energy E_{kin}. Assuming that every electron whose kinetic energy exceeds the band gap energy ΔE immediately produces another free electron through impact ionization,[10,19] we obtain that the average kinetic energy of all free electrons is approximately ΔE/2. The total energy carried by a free electron is thus ≈(3/2)ΔE = 9.75 eV = 1.56×10^{-18} J. In femtosecond plasmas, very little energy is transferred from the free electrons to the water molecules during the laser pulse, because collisional losses during the pulse are small and the recombination time is in the picosecond range (see the $r(t)$ curves in figure 1). The energy density e of femtosecond plasmas can therefore easily be estimated by multiplying the free electron density with the average energy carried by a free electron:

$$e \approx r_{max}\ (3/2)\,\Delta E\ . \qquad (2)$$

The energy density required to heat water from room temperature (20°C) to the boiling point is 335 Jcm^{-3}. Eq. (2) yields that this energy density corresponds to a free electron density of 2.15×10^{20} cm^{-3}. The complete vaporization enthalpy of 2590 Jcm^{-3} for water at ambient pressure (including the latent heat of vaporization) corresponds to a free electron density of 1.66 ×10^{21} cm^{-3}. The actual threshold for bubble formation will probably lie between these extremes, as does the critical electron density r_{cr} = 10^{21} cm^{-3} used in this study to define the breakdown threshold for femtosecond pulses. The above estimate confirms that one can generate laser effects without bubble formation by applying femtosecond pulses with a peak irradiance below the breakdown threshold.

The first experimental evidence for the possibility of multiphoton-induced heating of water to a level below the threshold of bubble formation has been provided by us in previous experiments with a numerical aperture of 0.25.[10, 21] At high irradiance (I/I_{th} = 200, t = 100 fs, l = 580 nm), a region with altered refractive index was observed *upstream* of the laser-induced cavitation bubble (Figure 3). In this region, the electron density and the corresponding energy density are obviously too low to cause bubble formation such as in the focal region further downstream, but the energy deposition via formation of free electrons is strong enough to be detected experimentally.

The model predictions in figure 2 for r_{max} at suprathreshold irradiance ($I > I_{rate}$) need to be interpreted with care, because above the threshold plasma is produced also upstream of the focal region[17,22,23] (see figure 3). Our model does not consider the shielding effects of these plasma parts and therefore overestimates the electron densities reached at the beam waist for $I > I_{rate}$. Besides the plasma shielding, the attainable electron density is limited also by the fact that for

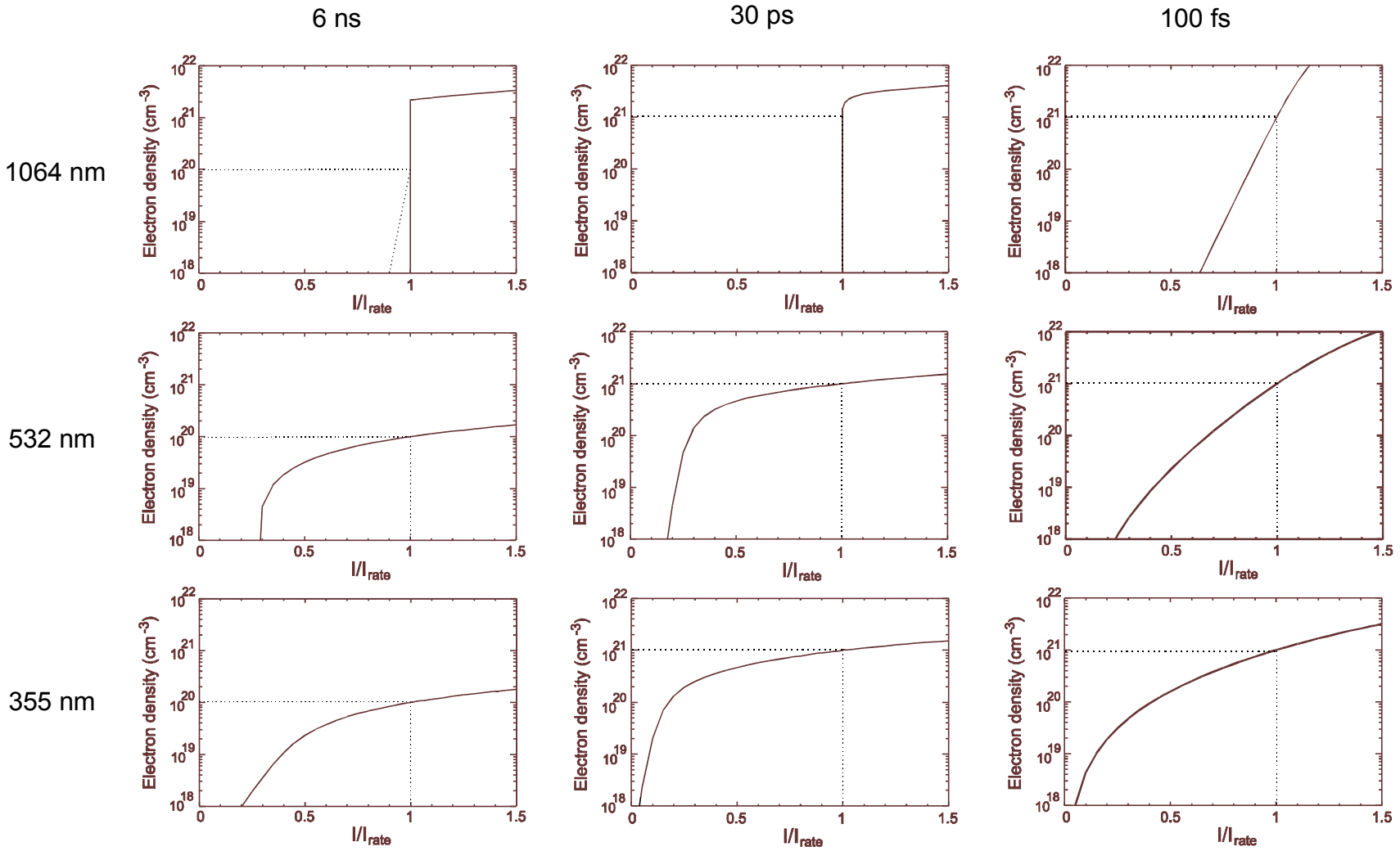

Figure 2: Maximum free electron density as a function of irradiance for different pulse durations and wavelengths. The calculations were performed for laser pulses focused into pure water at NA = 1.3. The horizontal axes have been normalized to the threshold irradiance I_{rate}. The threshold I_{rate} and the corresponding maximum electron density are marked by dotted lines.

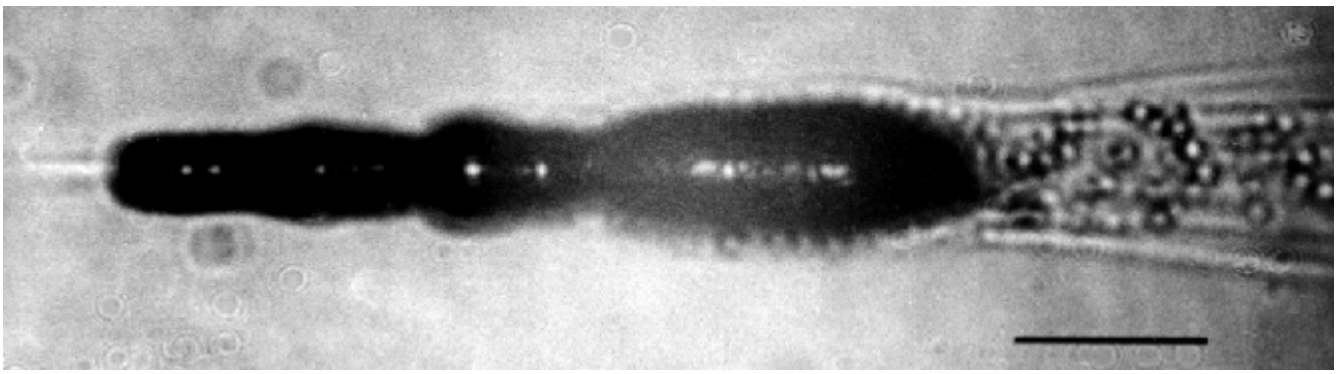

Figure 3: Optical breakdown region after focusing a 100 fs pulse with 35 µJ pulse energy into distilled water (λ = 580 nm, NA = 0.25, I/Ith = 200). The picture was taken 2 µs after breakdown, the bar represents a length of 100 µm. The laser light was incident from the right. The elongated dark structure is the cavitation bubble in its early stage of expansion. The Schlieren upstream of the cavitation bubble represent refractive index variations indicating a temperature rise. In this region, a low density plasma has been formed. The energy deposition during optical breakdown in this plasma region is just high enough to cause a detectable temperature rise, but too low to cause vaporization and bubble formation. The picture was slightly defocused to visualize the refractive index changes.

$$r = w^2 m_e e_o, \tag{3}$$

the plasma becomes both highly absorbing and reflective.[24] Here w denotes the angular frequency of the laser light, m_e the electron mass, and e_o the vacuum dielectric constant. The reflection of the incoming laser light by the plasma prevents an effective coupling of the light energy into the focal region and thus limits a further increase of the electron density.

3.5 Strategies for the refinement of laser dissection and cell manipulation

3.5.1 Strategies based on optical breakdown

Pulsed microirradiation systems presently available on the market employ nanosecond pulses at UV, visible or near IR wavelengths. It is obvious from the data in Table 4 that pulsed microirradiation techniques relying on optical breakdown can be refined by employing femtosecond pulses instead of nanosecond pulses because the breakdown threshold E_{rate} is 350-2600 times lower at 100 fs pulse duration than at 6 ns, and it amounts to only 0.6-4 nJ. Another factor contributing to the high precision achievable with femtosecond pulses is that a smaller percentage of the absorbed light energy is converted into mechanical energy than with nanosecond pulses. We found in previous experimental investigations at NA = 0.25 that the conversion rate from absorbed light energy into shock wave and cavitation bubble energy is about 90% for pulses with 6 ns duration but less than 15% for femtosecond pulses.[21]

The mechanical effects are more intense with longer pulse durations because the energy density in the focal region does not only depend on the free electron density reached during the laser pulse but also on the laser pulse duration. During a femtosecond pulse, only one 'set' of free electrons is generated which recombines after the end of the laser pulse. During nanosecond laser pulses, in contrast, free electrons are continuously created and recombine again, thus transferring a much larger amount of energy to the medium. The total energy transfer through collisions of free electrons with heavy particles is, as well, proportional to the pulse duration. Energy density, temperature and pressure are, as a result, much higher in nanosecond plasmas than in femtosecond plasmas, and the strength of the mechanical effects driven by the plasma expansion increases accordingly[10, 21, 25, 26].

Strong mechanical effects are for some microirradiation techniques not disadvantageous but rather desired. Examples are laser pressure catapulting[4,5] and optoporation of a relatively large number of cells with a few laser pulses.[8] For these applications, ns pulses with energies of a few microjoules are probably more suitable than ultrashort pulses with energies in the nanojoule range. The precision of laser dissection will certainly benefit from the use of ultrashort pulses with small single pulse energies, particularly when dissections inside of vital cells are intended. In cases where thick samples have to be prepared for further gene and protein analysis, a high precision can be achieved by applying a series of femtosecond or picosecond pulses with small single pulse energy and high repetition rate.

3.5.2 Strategies based on the generation of low-electron density plasmas

A particularly interesting result of our study is that femtosecond pulses enable the production of low-density plasmas with energy densities below the threshold for bubble formation. The biological effects of the low-density plasmas should be restricted to the focal region of the laser beam - or even to a fraction of this region where the irradiance is high enough to produce the electron density required to induce the biological effect of interest.

Experimental evidence that low density plasmas may play a role in cellular surgery with femtosecond pulses can be deduced from results published recently by König et al..[27] Using a series of laser pulses with 170 fs duration and 800 nm wavelength focused at NA = 1.3, they were able to cut chromosomes inside the cell nucleus of a vital cell without membrane damage and loss of vitality. They employed an irradiance of 10^{12} Wcm^{-2} which is about 1/5 of the irradiance predicted by our model for optical breakdown leading to bubble formation (table 3).

The working mechanism of cell manipulation through low-density plasmas still needs to be clarified. Potential working mechanisms are the temperature rise in the focal region as demonstrated in figure 3, chemical changes caused by the interaction of the free electrons with biological molecules, and thermoelastic stresses caused by the large temperature gradients induced in the focal region.[28] It is conceivable that thermoelastic stresses in conjunction with a mechanical weakening of biological structures caused by chemical changes are the basis of nanodissection.

To make optimum use of low-density plasmas for cell manipulation, one needs pulse durations and wavelengths which exhibit a large "tuning range" of the irradiance (or pulse energy, respectively) for a given variation in electron density. A large tuning range is indicated by a small slope in the r_{max} (I/I_{rate}) curves at $I < I_{rate}$. (see Fig. 2). We find this, in particular, for ultrashort pulse durations and short wavelengths.

It is interesting to note that the r_{max} (I/I_{rate}) curves for nanosecond pulses at 355 nm wavelength also have a small slope. This feature is a result of the large role of multiphoton processes at the UV wavelength (see figure 1) where only two photons are necessary to produce a free electron. The weak dependence of r_{max} on irradiance suggests that is might be possible to produce laser effects below the threshold for bubble formation with UV ns pulses, for example from a nitrogen laser at 337 nm, or from a frequency-tripled Nd:YAG laser. One needs to keep in mind, however, that the energy density in the focal region does not only depend on the free electron density but also on the laser pulse duration. For nanosecond pulses a lower electron density is required to keep the plasma energy density below the threshold for bubble formation than for femtosecond pulses.

In conclusion: Our numerical simulations revealed a possible new regime of laser tissue interaction: the creation of photochemical and photo'thermal' effects via free electron generation through nonlinear absorption. This regime had not been explored previously. Careful experimental investigations are now required to validate the model predictions and to answer the questions for which laser parameters and in which 'tuning range' one can produce laser effects below the threshold for bubble generation. On that basis one can then explore the kind and extent of the biological effects of low-density plasmas, and their potential applications.

Besides noninvasive surgery in living cells on a nanometer scale, the investigation of low-density plasmas is probably also important for multiphoton microscopy. Since multiphoton microscopy relies on multiphoton absorption, the irradiance levels used are not far from the optical breakdown threshold. Investigation of the formation of free electrons below the threshold for bubble formation will help in defining standards for the safe use of multiphoton microscopy on living systems.

REFERENCES

1. M. W. Berns, J. Aist, J. Edwards, K. Strahls, J. Girton, P. McNeill, J. B. Rattner, M. Kitzes, M. Hammer-Wilson, L. H. Liaw, A. Siemens, M. Koonce, S. Peterson, S. renner, J. Burt, R. Walter, P. J. Bryant, D. van Dyk, J. Coulombe, T. Cahill, and G. S. Berns, "Laser microsurgery in cell and developmental biology," *Science* **213**, 505-513, 1981.
2. M. W. Berns, W. H. Wright, R. Wiegand-Steubing, "Laser-microbeams as a tool in cell biology," *Int. Rev. Cytol.* **129**, 1-44, 1991.
3. K. O. Greulich, *Micromanipulation by Light in Biology and Medicine*, Birkhäuser Verlag, Basel, 1999.
4. M. Schindler, "Select, microdissect, and eject," *Nature Biotechnol.* **16**, 719-720, 1998

5. K. Schütze and G. Lahr, "Identification of expressed genes by laser-mediated manipulation of single cells," *Nature Biotechnol.* **16**, 737-742, 1998.
6. T. B. Krasieva, C. F. Chapman, V. J. Lamorte, V. Venugopalan, M. W. Berns, and B. J. Tromberg, "Cell permeabilization and molecular transport by laser microirradiation," *Proc. SPIE* **3260**, 38-44, 1998.
7. C. E. Sims, G. D. Meredith, T. B. Krasievy, M. W. Berns, B. J. Tromberg, and N. L. Albritton, "Laser-micropipet combination for single cell analysis," *Analyt. Chem* **70**, 4570-4577, 1998.
8. J. S. Soughayer, T. Krasieva, S. C. Jacobson, M. Ramsey, B. C. Tromberg, and N. Albritton, "Characterization of cellular optoporation with distance," *Analyt. Chem* **72**, 1342-1347, 2000.
9. A. Guerra, V. Venugopalan, K. Nahen, and A. Vogel, "Experimental investigation of optical breakdown using nanosecond 532- and 1064-nm laser pulses delivered at high numerical aperture," *Proc. SPIE* **4260** (this volume), 2001.
10. J. Noack and A. Vogel, "Laser-induced plasma formation in water at nanosecond to femtosecond time scales: Calculation of thresholds, absorption coefficients, and energy density," *IEEE J. Quantum Electron.* **35**, 1156-1167, 1999.
11. F. Docchio, C. A. Sachhi, and J. Marshall, "Experimental investigation of optical breakdown thresholds in ocular media under single pulse irradiation with different pulse durations," *Lasers Ophthalmol*. **1**, 83-93, 1986.
12. C. A. Sacchi, "Laser-induced electric breakdown in water," *J. Opt. Soc. Am. B*. **8**, 337-345, 1991.
13. F. Williams, S. P., Varama, and S. Hillenius, "Liquid water as a lone-pair amorphous semiconductor," *J. Chem. Phys.* **64**, 1549-1554, 1976.
14. J. F. Ready, *Effects of High Power Laser Radiation,* Academic Press, Orlando, 1971, pp. 261-262.
15. Y. R. Shen, *The Principles of Nonlinear Optics*, Wiley, New York, 1984.
16. N. Bloembergen, "Laser-induced electric breakdown in solids," *IEEE J. Quantum Electr.* **QE-10**, 375-386, 1974.
17. A. Vogel, K. Nahen, and D. Theisen, "Plasma formation in water by picosecond and nanosecond Nd:YAG laser pulses - Part I: Optical breakdown at threshold and superthreshold irradiance," *IEEE J. Selected Topics Quantum Electron.* **2**(4), 847-860, 1996.
18. D. X. Hammer, R. J. Thomas, G. D. Noojin, B. A. Rockwell, P. A. Kennedy, and W. P. Roach, "Experimental investigation of ultrashort pulse laser-induced breakdown thresholds in aqueous media," *IEEE J. Quantum Electr*. **QE-3**, 670-678, 1996.
19. P. K. Kennedy, "A first-order model for computation of laser-induced breakdown thresholds in ocular and aqueous media: Part I - Theory," *IEEE J. Quantum Electron*. **QE-31**, 2241-2249, 1995.
20. A. Vogel: *Optical Breakdown in Water and Ocular Media and ist Use for Intraocular Photodisruption*, Shaker, Aachen, 2001 (in press)
21. A. Vogel, J. Noack, K. Nahen, D. Theisen, S. Busch, U. Parlitz, D. X. Hammer, G. D. Nojin, B. A. Rockwell, and R. Birngruber, "Energy balance of optical breakdown in water at nanosecond to femtosecond time scales," *Appl. Phys. B* **68**, 271-280, 1999.
22. K. Nahen and A. Vogel, "Plasma formation in water by picosecond and nanosecond Nd:YAG laser pulses -- Part II: Plasma transmission, scattering and reflection," *IEEE J. Selected Topics Quantum Electron*. **2**, 861-871, 1996.
23. F. Docchio, P. Regondi, M. R. C. Capon, and J. Mellerio, "Study of the temporal and spatial dynamics of plasmas induced in liquids by nanosecond Nd:YAG laser pulses. 2: Plasma luminescence and shielding," *Appl. Opt.* **27**, 3669-3674, 1988.
24. T. P. Hughes, *Plasmas and Laser Light*, Adam Hilger, Bristol, 1975.
25. E. J. Chapyak, R. P. Godwin, and A. Vogel, "A comparison of numerical simulations and laboratory studies of shock waves and cavitation bubble growth produced by optical breakdown in water," *Proc. SPIE* **2975**, 335-342, 1997.
26. A. Vogel, S. Busch, and U. Parlitz, "Shock wave emission and cavitation bubble generation by picosecond and nanosecond optical breakdown in water," *J. Acoust. Soc. Am.* **100**, 148-165, 1996.
27. K. König, I. Riemann, P. Fischer, and K. Halbhuber, "Intracellular nanosurgery with near infrared femtosecond laser pulses," *Cell. Mol. Biol.* **45**, 195-201, 1999.
28. I. Itzkan, D. Albagli, M. L. Dark, L. T. Perelman, C. v. Rosenberg, and M. S. Feld, "The thermoelastic basis of short pulsed laser ablation of biological tissue," *Proc. Natl. Acad. Sci. USA* **92**, 1960-1964, 1995.